The International Journal of Advanced Manufacturing Technology (2022) 120:5741–5754
https://doi.org/10.1007/s00170-022-09000-x

ORIGINAL ARTICLE

Experimental validation and numerical simulation of flexible and microscale roll gap control technology

Tingsong Yang[1,2] · Qifa Chen[1,2] · Yanfeng Feng[3] · Yang Hai[1,2] · Fengshan Du[1,2]

Received: 7 August 2021 / Accepted: 28 February 2022 / Published online: 2 April 2022

Abstract

This paper proposes a new flexible and microscale roll gap control technology to obtain a stronger strip flatness control ability. According to the principle of microscale roll gap control technology, an electromagnetic control rolling mill with the function of roll profile control and large diameter ratio rolling is designed and built. To analyze the flatness control ability, a comprehensive finite element model (FEM) is established, and an indentation experiment and a rolling experiment are carried out. The simulation results show that under different rolling forces and tensions, the average quadratic crown control ability is more than 40 μm, and the average quartic crown control ability is more than − 3 μm. The control ability increment of the quadratic crown is greater than that of the quartic crown. In the indentation experiment, a stable roll profile can be achieved by PID control after reaching the target roll profile. Increasing the regulation amount can change the strip crown from positive to negative. Even under high rolling force conditions, microscale roll gap control technology can also realize a strip crown adjustment of 19.5 to 0.5 μm. Moreover, this technology can adjust the strip shape from edge waves to non-waves and middle waves in the rolling experiment. In this paper, the feasibility of using this technology to adjust the roll gap shape has been verified, and we demonstrate that the roll gap control goal of uniform transverse size distribution can be achieved.

Keywords Microscale roll gap control technology · Electromagnetic control rolling mill · Electromagnetic control roll · Strip flatness control · Roll gap shape

1 Introduction

Adjusting a uniform roll gap is the core of solving the strip flatness problem. Because of the roll deflection and roll flattening, it is difficult to form a uniform roll gap. To solve this problem, different strip flatness control technologies are proposed. According to different control principles, these technologies can be divided into roll deformation control, initial roll profile control, and displacement roll profile control.

In the field of roll deformation control, Cao et al. [1] proposed that the quadratic crown of the strip can be decreased nearly linearly with increasing bending force in a 6-high cold rolling mill. Ogawa et al. [2] proposed that the control ability of intermediate roll bending is stronger than that of working roll in a 12-high cluster mill. Wang et al. [3] proposed that the coordination utilization of nonsymmetrical work roll bending control and tilting roll control has the flatness control ability to adjust the single side edge waves in the 6-high universal crown mill. Wang et al. [4, 5] proposed a simulation approach to obtain actuator efficiency factors in terms of roll bending and roll shifting and an improved approach that can predict the location of the flatness defect. Aljabri et al. [6] found that the combined use of working roll crossing and shifting can adjust the flatness problem of asymmetric rolling. The above studies show that the roll gap control abilities of roll deformation control mainly focus on low-order wave problems. For high-order wave problem, it is necessary to adopt a combination of different flatness control technologies, but this method is difficult. Therefore, initial roll

✉ Fengshan Du
fsdu@ysu.edu.cn

1 National Engineering Research Center for Equipment and Technology of Cold Strip Rolling, Yanshan University, Qinhuangdao 066004, Hebei, People's Republic of China

2 College of Mechanical Engineering, Yanshan University, Qinhuangdao 066004, Hebei, People's Republic of China

3 College of Mechatronics and Control Engineering, Shenzhen University, Shenzhen 518060, Guangzhou, People's Republic of China

profile control has been proposed to improve the control ability of adjusting the high-order wave problem.

In the field of initial roll profile control, Lu et al. [7] designed a new third-order CVC roll profile to reduce the axial force on the work roll. Li et al. [8] suggested that the contour angle is the key factor in SmartCrown technology. In addition, Li et al. [9] proposed a design method of quartic CVC roll profiles that has better flatness control ability. Linghu et al. [10] established a 3D FEM of a 6-high CVC rolling mill to investigate the flatness control capability. Fei et al. [11] proposed a new method for designing CVC roll profiles. Cao et al. [12] found that a varying contact-length backup roll (VCR) can expand the strip crown control range and improve the roll gap stiffness. Wang et al. [13] designed an edge variable crown (EVC) roll profile that can control the edge drop. Li et al. [14] designed a new asymmetrical self-compensating work roll (ASR) that has a better control ability under the influence of roll wear. Cao et al. [15] developed an integrated design of roll contours for EDW and matched VCR, which can be used to solve the strip edge drop problem. In practical applications, the above technologies have achieved different control effects. However, the design of a new roll profile requires many calculations, and designers are required to perfect the design.

Given the above problems, displacement roll profile control is proposed. Sumitomo Metal Industries [16] proposed a roll thermal-bulging technology. In this technology, electrical sticks are installed in the roll inner hole, and the roll is heated to bulge. Arif et al. [17] analyzed the influence of the thermal–mechanical load on the roll profile and the rolled strip thickness. Masui et al. [18, 19] developed a variable crown (VC) roll with an arbor and a sleeve, which can control the strip profile by regulating the oil pressure. Zhang et al. [20] analyzed the shape control performance of a dynamic shape roll (DSR) rolling mill to study the vertical asymmetry problem. These technologies can directly change the roll gap of the strip flatness defect area. However, thermal-bulging technology has low heating efficiency and thermal control difficulty. The bulging pressure of VC or DSR is limited due to the hydraulic oil seal, and the roll shell needs to be explicitly designed to avoid crushing. Based on the thermal force control principle, roll profile electromagnetic control technology (RPECT) is proposed [21]. RPECT uses the thermal expansion of the electromagnetic stick (ES) and the thermal necking of the electromagnetic control roll (ECR). A significant contact pressure can be generated between the ECR and ES, which can change the ECR roll profile. Liu et al. [22] proposed the optimized structure of ES. Feng et al. [23] designed a large nested electromagnetic control roll and analyzed its control ability. However, the above studies are mainly based on the off-line roll, and the effectiveness in the on-line process has not yet been verified.

In this paper, a microscale roll gap control technology is proposed based on roll profile electromagnetic control. Compared with other technologies, this technology has flexible roll gap shape control ability and high transverse stiffness. To verify the flatness control ability, microscale roll gap control technology is equipped on a single-roll-driven asymmetric strip rolling mill. A comprehensive finite element model (FEM) is established and verified. It includes an FEM for predicting the electromagnetic control roll profile and an FEM of the rolling process. Based on the FEM, this paper compares and studies the influence of the ECR roll crown on the roll gap shape under different rolling forces and tension conditions. This paper also carries out an indentation experiment and a rolling experiment on an electromagnetic control rolling mill and discusses the ECR roll profile stability, roll gap shape control ability, and effect of the electromagnetic rolling mill.

2 Principle of the microscale roll gap control technology and FE model

2.1 Principle of the microscale roll gap control technology

The electromagnetic control rolling mill can be divided into two asymmetrical roll systems. The upper roll system includes two supporting rolls and one working roll, and the lower roll system is an ECR that can be used to control the roll profile. The diameter ratio between the lower working roll and the upper working roll is 3.375. Due to the large diameter ratio, the bending of the upper working roll is larger than that of the lower working roll. If microscale roll gap control technology is not applied, then the edge roll gap value is less than the middle value, which leads to an instability in the strip edge extension and the edge wave problem. The principles of microscale roll gap control technology are shown in Fig. 1. The ECR roll crown can be increased by controlling and then compensating for the deflection of the upper working roll to eliminate flatness problems. If the ECR roll crown is continuously increased, then the middle roll gap value can be less than that on the edge, which leads to the instability of the strip middle elongation and the middle wave problem. Therefore, the strip flatness can be controlled from the double edge wave to the non-wave, and then to the middle wave, which indicates that the mill has flatness control ability and can achieve the goal of flatness defect adjustment.

2.2 FEM of the microscale roll gap control technology

Microscale roll gap control technology involves the calculation of the electromagnetic field, temperature field, and stress field. Due to the large calculation amount of the

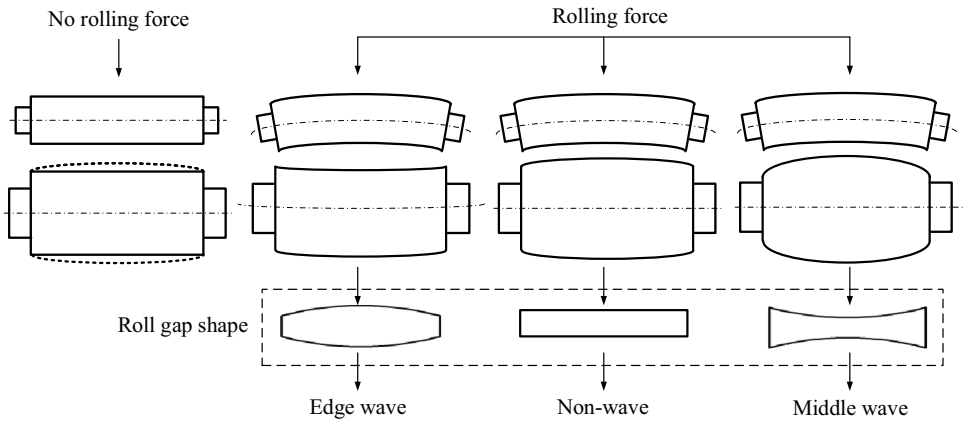

Fig. 1 Flatness problems and control principle of microscale roll gap control technology

multifield coupling problem, it is difficult to calculate the finite element model (FEM) with elastic plastic deformation and electromagnetic analysis. Therefore, the FEM needs to be simplified. In the traditional solving process, the roll gap is formed by the influence of the original roll profile, roll deflection, roll flattening, etc. Considering that the ECR roll profile is a steady-state roll profile in microscale roll gap control technology, it can be brought into the roll gap in the form of the origin roll profile. Therefore, the FEM of microscale roll gap control technology can be divided into two models, including an FEM of roll profile control and an FEM of the rolling process. The FE model of roll profile control is an electromagnetic-thermal-structure coupled model and can be used to obtain the ECR roll profile. The FEM of the rolling process is a three-dimensional model and can be used to analyze the rolling process.

2.2.1 FEM of the roll profile control

The FEM of the roll profile control is based on the electromagnetic-thermal-structure analysis module integrated by the MSC. Marc 2016. The model includes ES, ECR, induction coils, and air units, as shown in Fig. 2. ES, ECR, and induction coils have revolving structures, and the external boundaries and parameters also have axisymmetric characteristics. Therefore, this model can be simplified as an axisymmetric model. To improve the simulation accuracy, the outermost air units are set to the zero point of the magnetic and electric

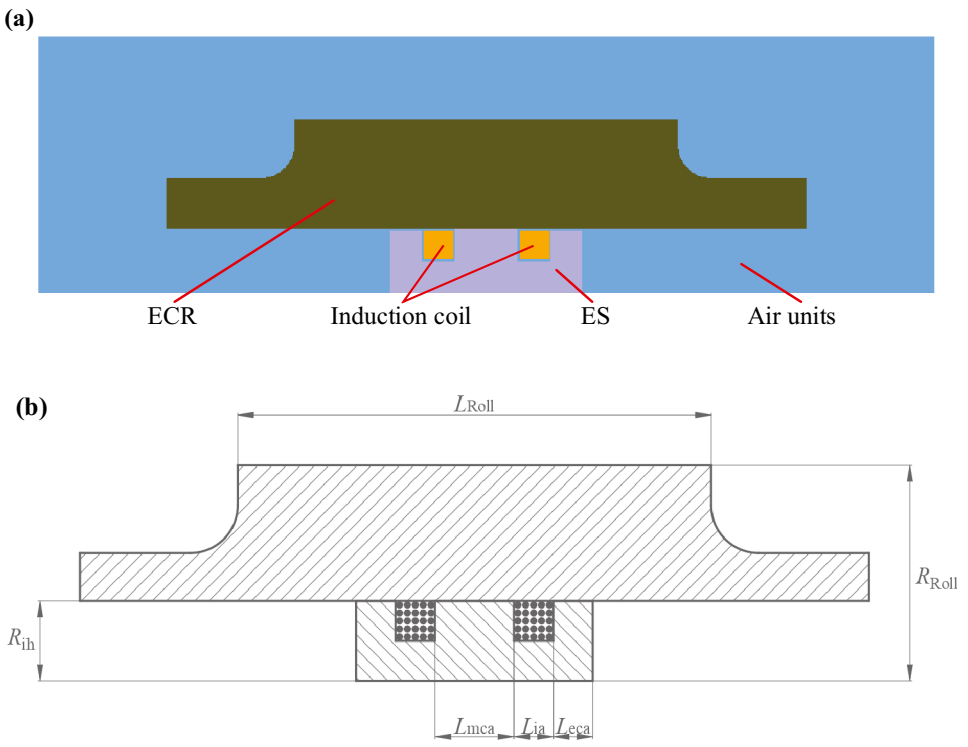

Fig. 2 FEM of ECR and parameter diagram. **a** FEM and **b** parameter diagram

Table 1 FEM parameters of the roll profile control

Name	Value	Name	Value
Roll radius (R_{Roll})	135 mm	Roll length (L_{Roll})	300 mm
Radius of the ECR inner hole (R_{ih})	50 mm	Length of ES (L_{ES})	150 mm
Length of the middle contact area (L_{mca})	50 mm	Length of the induction area (L_{ia})	25 mm
Length of the edge contact area (L_{eca})	25 mm	Material of ECR and ES	C45
Frequency of induction coils	400 Hz	Average current density	3 A/mm^2
Cross-sectional area of conductor	6 mm^2	Coil turn	25
Constant voltage	35 V	Ambient temperature	8.5 ℃
Control time	500 s	Temperature control method	PID

potentials. The heat transfer relationship between the ECR and ES is contact heat transfer, and the coefficient is 3 kW/(m^2·K) [24]. In addition to the heat transfer between the ECR and ES, the heat transfer relationships, which are ECR-air and ES-air, are air cooling, and the coefficient is 0.03 kW/(m^2·K) [25]. The FEM parameters are shown in Table. 1.

Considering the Curie point in electromagnetic induction, the electromagnetic property parameters of C45 with temperature are introduced into the FEM, as shown in Fig. 3.

The results in the literature [25] show that the FEM has a high simulation accuracy and can be used to predict the ECR roll profile. This paper does not repeat the relevant experiments to verify the FEM. When the ECR roll crown reaches the target value, the temperature control mode of the ES is changed to the intermittent heating or PID control mode, and then the target roll profile can be maintained. Therefore, the regulation method can keep the ECR roll profile stable and then control the ECR by the result of the model.

Figure 4 shows the roll profile curves at different times and the corresponding control methods after reaching the target roll profile. In Fig. 4a, because the roll profile curve is the curve of the middle bulge, the roll crown C_w, which is the difference between the middle bulging value and edge bulging value of the ECR, can be selected as the evaluation index. When the regulation time is changed from 170 to 420 s, the corresponding C_w is divided into 20 μm, 30 μm, and 40 μm. In Fig. 4b, the target roll profile can be achieved at 170 s, 270 s, and 420 s. After the roll profile is achieved,

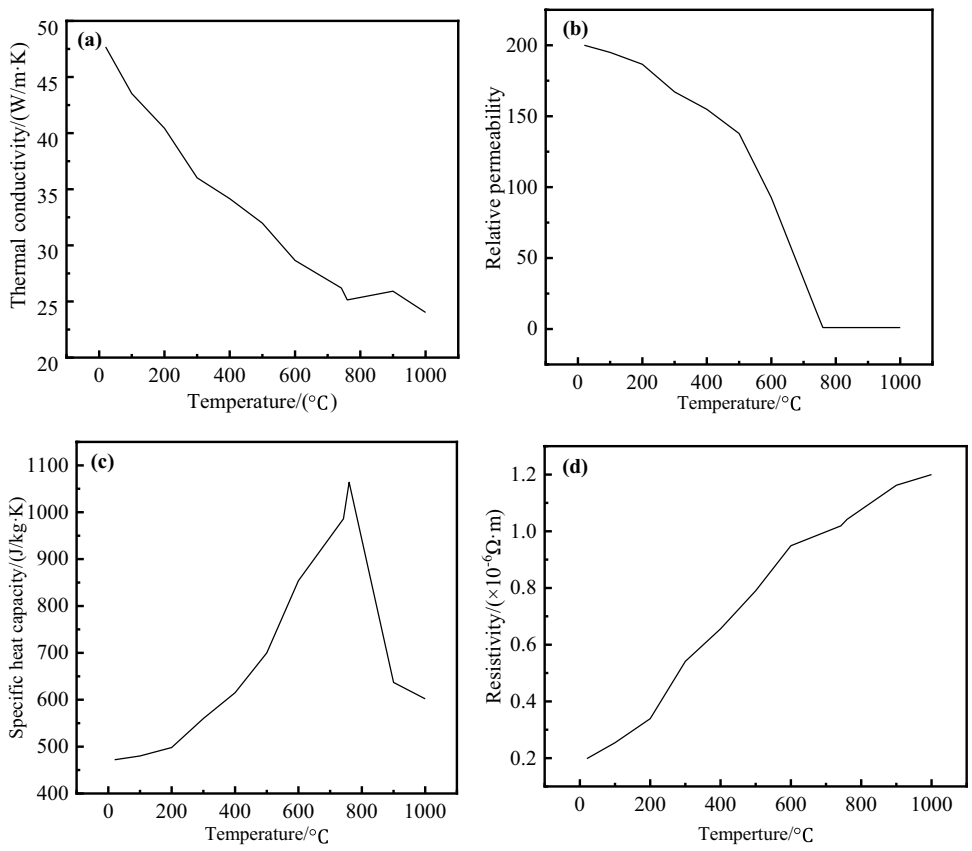

Fig. 3 The material parameters of C45. **a** Thermal conductivity, **b** relative permeability, **c** specific heat capacity, **d** resistivity

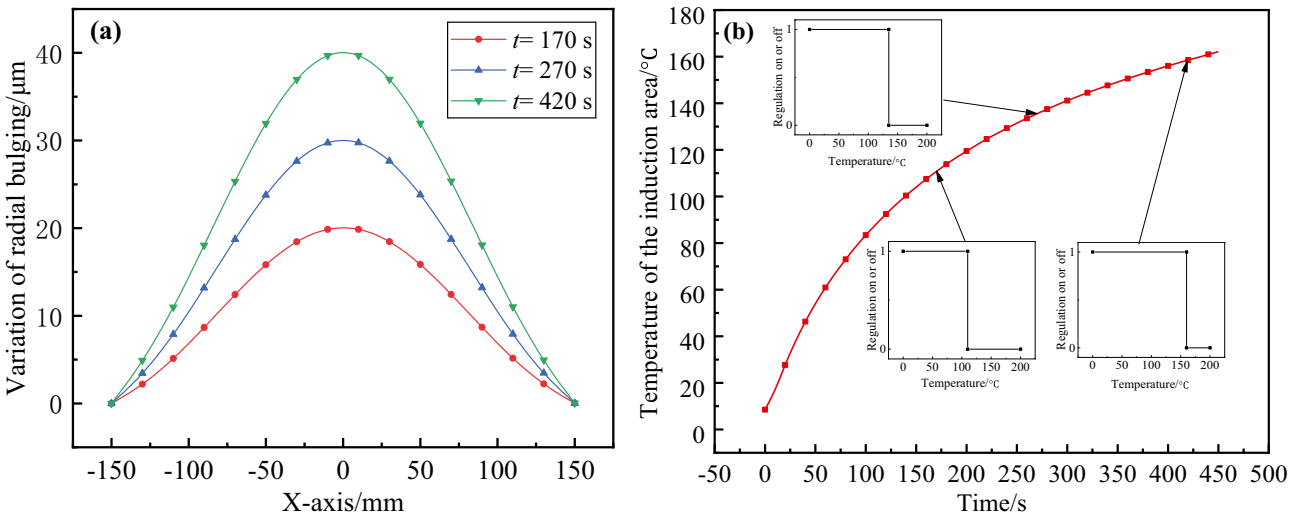

Fig. 4 Roll profile curves with different roll crowns and temperature control method of different cases. **a** Roll profile curves and **b** temperature control method

the temperature control method of the ES induction area is changed to the PID control mode, and the marked temperature of starting or stopping the power supply is the temperature corresponding to the time of forming every target roll profile. When the detected temperature of the ES induction area is higher than the marked temperature, the power supply can be stopped. Otherwise, the power supply is started.

2.3 FEM of the rolling process

Figure 5 shows the electromagnetic control rolling mill and the asymmetric roll system. The lower working roll is an ECR, and the ECR sizes are the same as those of the FEM of the roll profile control. The rolls are zero crown rolls. Therefore, the FEM of the rolling process can be simplified to a 1/2 model to reduce the calculation amount, as shown in Fig. 6.

The model element adopts a hexahedron element with eight nodes. Due to the elastic deformation in the rolling process, rolls and strips are deformable bodies. The rolling force is applied at the end of the backup rolls. The lower working roll is a driving roll, and the upper roll system adopts the driven mode. The contact relationship between the roll and strip is Coulomb friction. Through the tensile test, the stress–strain curve of 1060 Al is shown in Fig. 7. The FEM parameters of the rolling process are shown in Table. 2.

3 Results and discussion

To analyze the roll gap shape, the curve equation can be used to fit the roll gap. In this paper, the roll gap shape is mainly described by a quartic polynomial.

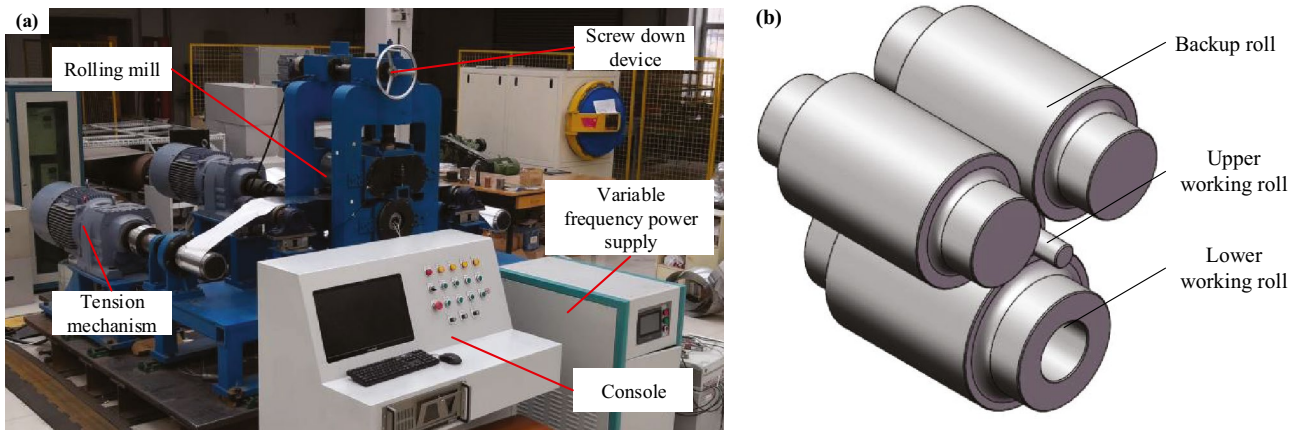

Fig. 5 Electromagnetic control rolling mill and asymmetric roll system. **a** Rolling mill and **b** asymmetric roll system

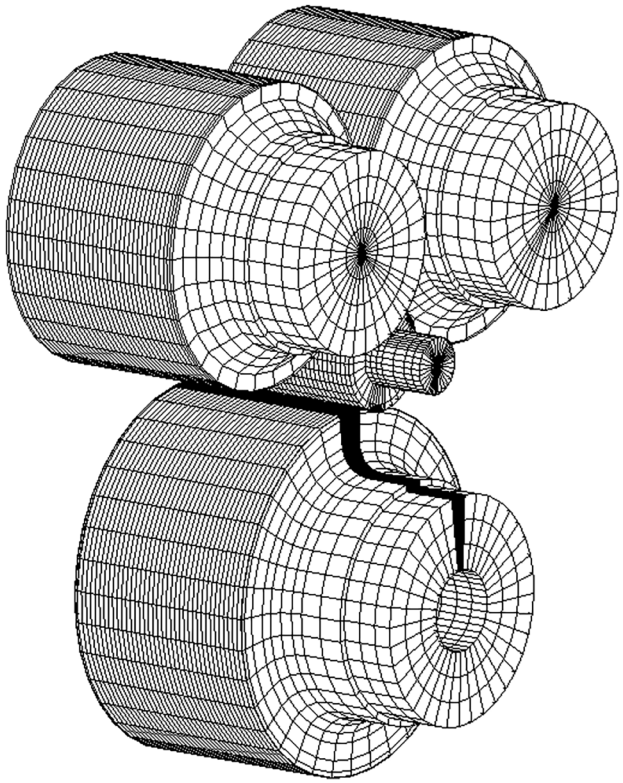

Fig. 6 FEM of the rolling process

$$f(x) = a_0 + a_2x^2 + a_4x^4, x \in [-1, 1] \tag{1}$$

where $f(x)$ is the shape curve of the loaded roll gap, x is the normalized strip width, and a_0, a_2, and a_4 are equation coefficients.

Corresponding to the strip wave, the loaded roll gap crown is decomposed into the quadratic crown and the quartic crown to evaluate the strip flatness control ability, which are C_{w2} and $C_{w4,}$ respectively.

$$\begin{cases} C_{W2} = -(a_2 + a_4) \\ C_{W4} = -a_4/4 \end{cases} \tag{2}$$

The quadratic crown can correspond to low-order wave problems, such as double edge waves and medium waves. The quartic crown can also correspond to high-order waves, such as the quarter wave and the edge middle composite wave.

3.1 Influence of the ECR roll crown on the roll gap shape

Figure 8 shows the variation in the roll gap shape under different rolling forces and different C_w. The roll gap value at the middle is taken as the reference and zeroed, and the transverse points of the roll gap are normalized. Under the same rolling force, the roll gap value at the edge can be increased from negative to positive with increasing C_w. Under the same C_w, the roll gap value at the edge can be decreased with increasing rolling force. Therefore, increasing C_w can improve the edge drop problem by roll deflection, and the improved ability can be weakened when the rolling force is increased. The reason is that a large rolling force has a large roll deflection, and the edge drop is serious. When C_w is increased, the roll gap value at the middle decreases, and that at the edge increases. If the roll gap value at the middle is equal to that at the edge, the thickness of the roll gap is uniform. Therefore, microscale roll gap control technology has edge wave control ability, and the control ability is affected by rolling force.

Figure 9 is the roll gap crown control region of changing C_w and the rolling force. Compared with the difference between Point A and Point B, increasing C_w can positively increase C_{w2} and inversely increase C_{w4}. Compared with the difference between Point B and Point D, increasing the rolling force can positively decrease C_{w2} and inversely increase

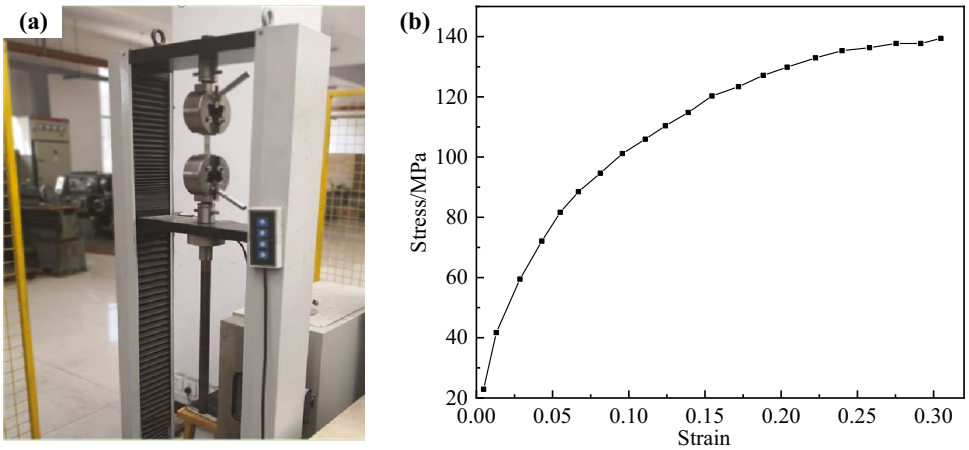

Fig. 7 Tensile test and stress–strain curve of 1060 Al. **a** Tensile test and **b** stress–strain curve

Table 2 FEM parameters of the rolling process

Parameter name	Value	Parameter name	Value
Backup roll diameter (D_B)	225 mm	Backup roll length	300 mm
Upper working roll diameter (D_{UW})	80 mm	Upper working roll length	300 mm
Lower working roll diameter (D_{LW})	270 mm	Lower working roll length	300 mm
The material of roll	C45	The material of strip	1060 Al
Rolling speed	100 mm/s	Friction coefficient	0.1
Rolling force	5 t, 10 t, 20 t	Strip width/thickness	250 mm, 0.5 mm
Elastic modulus of 1060 Al	70 GPa	Poisson's ratio of 1060 Al	0.33

C_{w4}. The adjustment effect of changing C_w is stronger than that of changing the rolling force. Otherwise, different rolling forces can also lead to a difference in the effect of changing C_w. When the rolling forces are 5 t and 20 t, the C_{w2} control ability of changing C_w is 45.21 μm and 36.04 μm, and the C_{w4} control ability is − 3.43 μm and − 3.18 μm. Therefore, under a larger rolling force, the C_{w2} control ability of changing C_w can be decreased, and the C_{w4} control ability can be increased slightly. However, changing the rolling force also changes the rolling condition, and the control strategy of changing only the rolling force cannot be used to control the strip flatness.

Specifically, the roll gap curves in Fig. 8c are different from those curves in Fig. 8a, b. The roll gap curves have bulging in the middle area and a depression 50 mm away from the middle area. To analyze the cause, Fig. 10 shows the strip lateral displacement and the roll gap curve of $C_w = 0$ μm in Fig. 8c. Due to the symmetry, the direction from the middle area to the edge area is selected as the positive direction of the metal transverse flow. When the roll gap is in good condition, the metal transverse flow usually shows a monotonic change. However, the results in Fig. 10 show that the negative flow range is 0 ~ 35 mm and 110 ~ 120 mm, and the positive flow range is 35 ~ 110 mm. The metal has an uneven transverse flow and results in the fluctuation of the roll gap shape variation. The reason is that the roll deflection can be increased with increasing rolling force, and the roll gap size is not uniform in the transverse direction. Then, the metal can flow laterally to the large area. In Fig. 10, there are two large areas, including the middle area and the position 80 mm away from the middle area. The reason for the former is that the roll deflection makes the metal flow

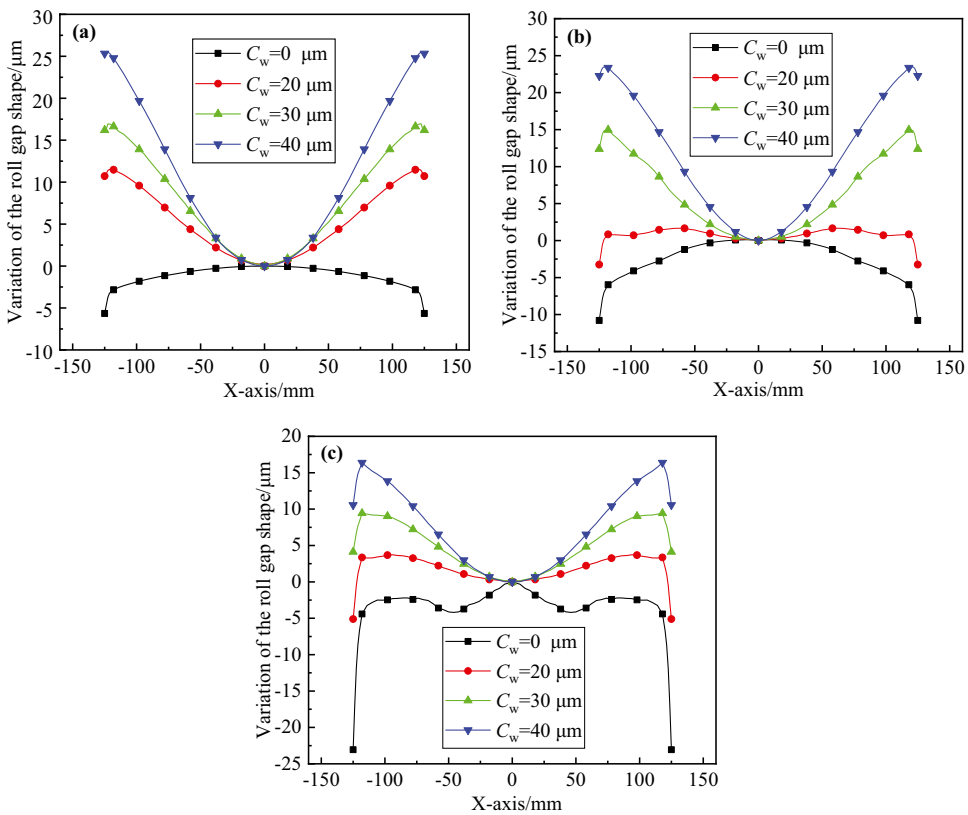

Fig. 8 Variation in the roll gap shape under different C_w and different rolling forces. Rolling force is **a** 5 t, **b** 10 t, and **c** 20 t

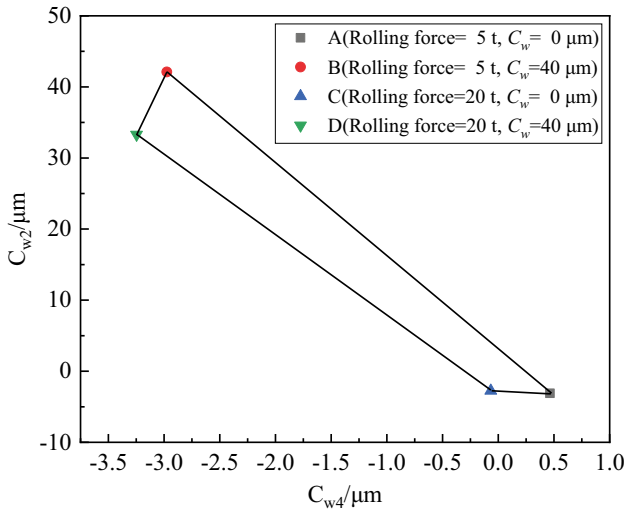

Fig. 9 Roll gap crown control region of changing C_w and the rolling force

towards the middle. The reason for the latter is that, affected by the strip before and after rolling, the metal in the edge cannot completely flow to the middle and accumulates at the 80 mm position.

Figure 11 shows the metal transverse displacement when C_w is different and the rolling force is 20 t. When C_w is 20 μm, the lateral displacements at [40 mm, 125 mm] increase positively, and the metal moves towards the strip edge. When C_w is 30 μm, the lateral displacement at [0 mm, 30 mm] is almost zero, and the lateral displacement at [30 mm, 125 mm] begins to increase gradually. When C_w is 40 μm, there is no negative displacement at points in the whole strip width range. Therefore, microscale roll gap control technology can effectively control the roll gap shape by changing C_w. When the roll gap size is not uniform due to excessive rolling force, the metal transverse flow state can be changed by adjusting the ECR roll profile.

3.2 Influence of the tension condition on the roll gap shape

In addition to the rolling force, tension is also a crucial parameter in the rolling process. In this paper, the front and back tensions are the same, and the value ranges from 0 to 30 MPa. Figure 12 shows the variation in the roll gap shape under different C_w and different tensions. The variation trend of the roll gap shape is like that in Fig. 8. Under the same tension, the roll gap value can be increased with increasing C_w. Under the same C_w, the roll gap value is also improved with increasing tension. However, the influence of the tension is weaker than that of the ECR roll crown. The reason is that the front and back tension, in this paper, is uniformly distributed tension and is also the preset tension before rolling. It has a weak lateral adjustment ability on the strip rolling process. The transverse effect of tension on strip elongation is weaker than that caused by changing C_w.

Figure 13 is the roll gap crown control region of changing C_w and the tension. Compared with the difference between Point A and Point B, increasing C_w can positively increase C_{w2} and inversely increase C_{w4}. Compared with the difference between Point B and Point D, increasing the tension can positively decrease C_{w2} and inversely increase C_{w4}. Changing the tension and changing C_w have interactive effects on the flatness control. When the tensions are 10 MPa and 30 MPa, the C_{w2} control abilities of changing C_w are 44.47 μm and 43.92 μm, and the C_{w4} control abilities are − 3.75 μm and − 3.25 μm. When C_w is 0 μm

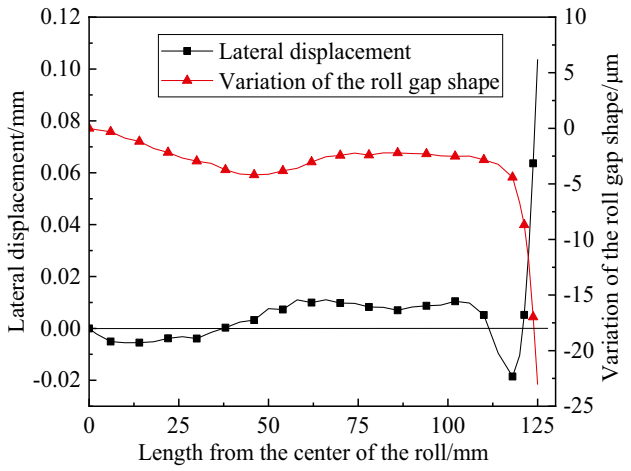

Fig. 10 Variation in the loaded roll gap shapes and lateral displacement of the strip when C_w is 0 μm and the rolling force is 20 t

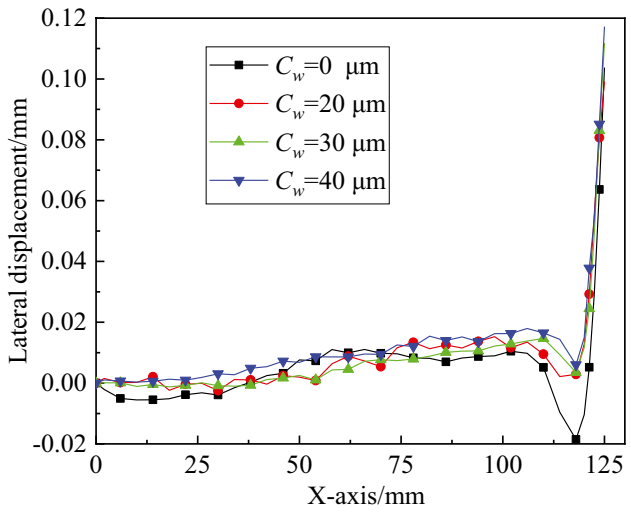

Fig. 11 Variation in lateral displacement when C_w is different and the rolling force is 20 t

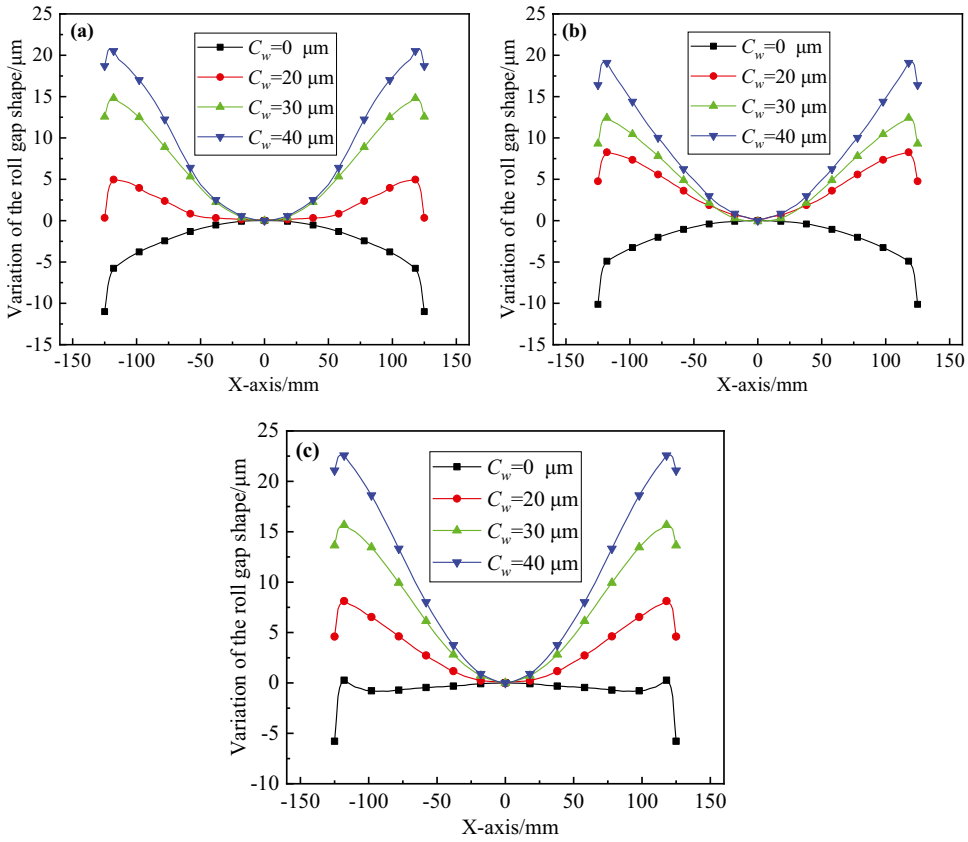

Fig. 12 Variation in the roll gap shape under different C_w and different tensions. Tension is **a** 10 MPa, **b** 20 MPa, and **c** 30 MPa

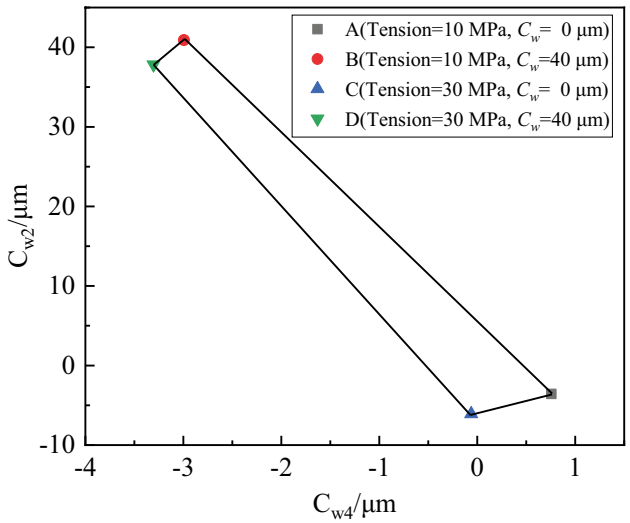

Fig. 13 Roll gap crown control region of changing C_w and the tension

and 40 μm, the C_{w2} control abilities of changing the tension are − 2.52 μm, − 3.07 μm, and the C_{w4} control abilities are − 0.82 μm, − 0.32 μm. Therefore, the adjustment effect of changing C_w is stronger than that of changing the tension.

4 Experiment and discussion

4.1 Indentation experiment

4.1.1 Experimental equipment and scheme

An indentation experiment is carried out to analyze the loaded ECR roll profile. The roll arrangement is shown in Fig. 14. The parameters of the electromagnetic control rolling mill are the same as those of the above FEM. Before the experiment, the ES needs to be heated to obtain the target roll profile. The strips are fed into the roll gap first, and then the rolling force is adjusted. After rolling for a certain distance, the indentation test is completed.

4.1.2 Experimental analysis of the ECR roll profile stability

According to the results in Fig. 8, the experimental rolling force can be selected from the range of 10 to 20 t. The indentation experiment conditions of the ECR roll profile stability are as follows: the rolling force is 15 t, the C_w is 30 μm, the continuous heating temperature of the ES induction area is 135 ℃, and the control method is PID control after the continuous heating temperature reaches 135 ℃. Otherwise,

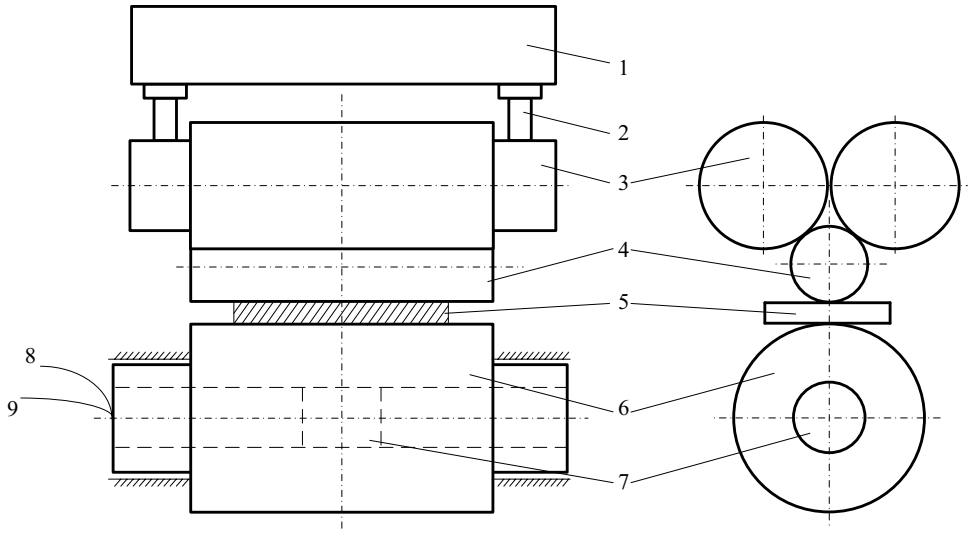

Fig. 14 The structural sketch of indentation experiment

the indentation experiment began when the temperature of the ES induction heating zone reached 135 ℃ and lasted for 600 s. The time interval of the strip feeding is 120 s.

Figure 15 shows the strip thickness distribution of the indentation experiment at different times. With time, the average thicknesses are 0.449 mm, 0.452 mm, 0.449 mm, 0.450 mm, and 0.447 mm. The reason for the average thickness difference is as follows: there is a certain rolling force fluctuation among the indentation experiments at different times, which further causes the average thickness fluctuation. However, overall, the average thickness fluctuation after the adjacent experiments is less than 5 μm. Therefore, the ECR roll crown can be kept stable for a certain period by PID control.

4.1.3 Experimental analysis of the roll gap shape control ability

The indentation experiment conditions of the roll gap shape control ability are as follows: C_w can be changed from 0 to 40 μm, and the rolling force can be changed from 10 to 30 t. Figure 16 shows the strip thickness distribution when C_w is changed and the rolling force is 10 t. With increasing C_w, the strip thickness distribution can be changed from "thin and thick edges" to "thick and thin middle edges." The central thickness of the rolled strip is 0.476 mm, 0.474 mm, 0.471 mm, and 0.468 mm, and the strip crown is 4 μm, 1.5 μm, − 3 μm, and − 9 μm. In some cases, the rolled strip crown is changed

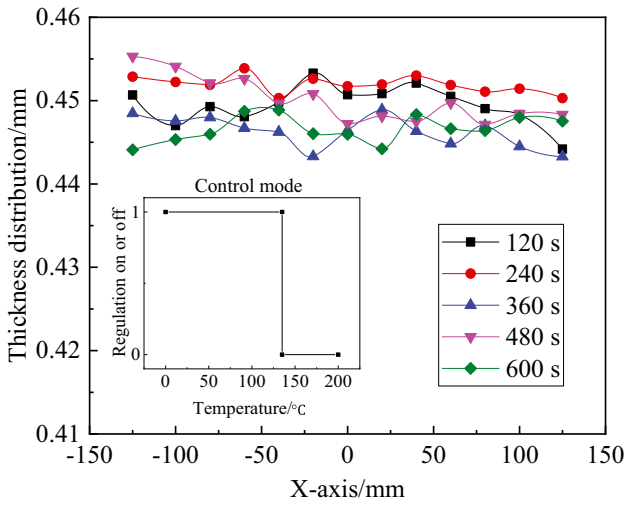

Fig. 15 Thickness distribution of the indentation experiment at different times

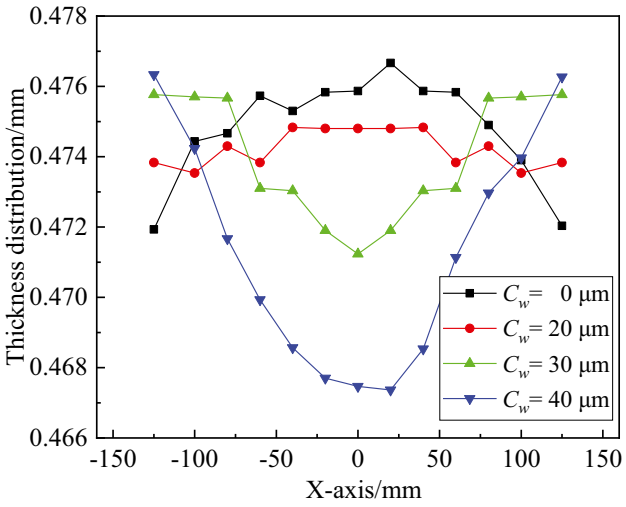

Fig. 16 Thickness distribution of the rolled strip when C_w is changed, and the rolling force is 10 t

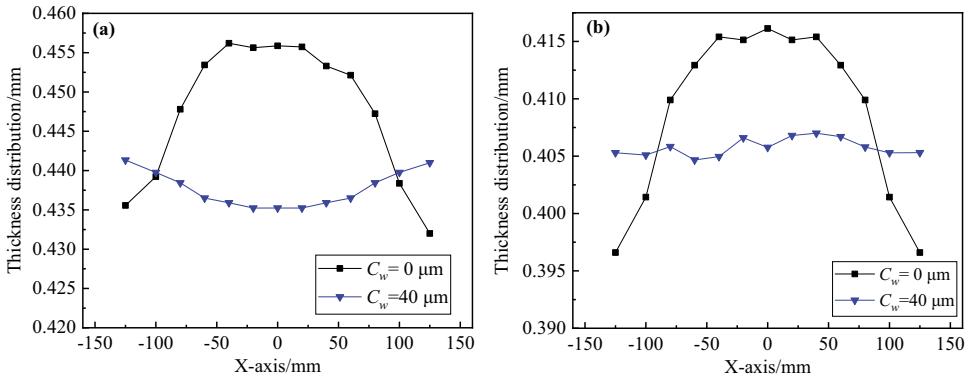

Fig. 17 Strip thickness distribution when C_w is 0 μm or 40 μm and the rolling force is different. Rolling force is **a** 20 t and **b** 30 t

from positive to negative. This shows that the microscale roll gap control technology has a good control effect on the roll gap.

Figure 17 shows the strip thickness distribution when the rolling force is changed, and the ECR roll crown is 0 μm or 40 μm. In Fig. 17a, with increasing C_w, the strip crown can be decreased from 20 to − 7.5 μm. In Fig. 17b, with increasing C_w, the strip crown can be decreased from 19.5 to 0.5 μm. The above results show that when C_w is 40 μm, the strip edge drop is solved, and the rolled strip has a good thickness distribution. Although the rolling force is increased, the variation in C_w is enough to compensate for the roll deflection, and the strip flatness can be adjusted by microscale roll gap control technology. Therefore, if a good thickness distribution needs to be obtained with a large rolling force, then the ECR roll crown needs to be further increased.

4.2 Strip rolling experiment

4.2.1 Experimental scheme

A rolling experiment is carried out to study the effect of microscale roll gap control technology on the rolling process. The scheme of the strip rolling experiment can be described as follows: before the experiment, the ES is heated by the power supply in advance, and then rolling can begin. The rolling speed is 100 mm/s, the rolling force is 15 t, the strip width is 250 mm, and the strip thickness is 0.5 mm. The tensions are 0 MPa, 20 Mpa, and 35 MPa, and C_w is 0 μm, 30 μm, and 40 μm.

4.3 Experimental analysis of tension condition

To select reasonable tension parameters, an experiment of variable tension rolling is carried out. Figure 18 shows the strip deformation under different tensions. When microscale roll gap control technology is not carried out, the rolled strip exhibits local waves and double edge waves. With increasing tension, the local waves have been significantly improved, and the width and height of the double edge wave have been decreased. When the tension is increased to 35 MPa, the local waves disappear, and the strip flatness can be significantly improved compared with the first two conditions. Therefore, 35 MPa can be selected as the tension parameter of the rolling experiment.

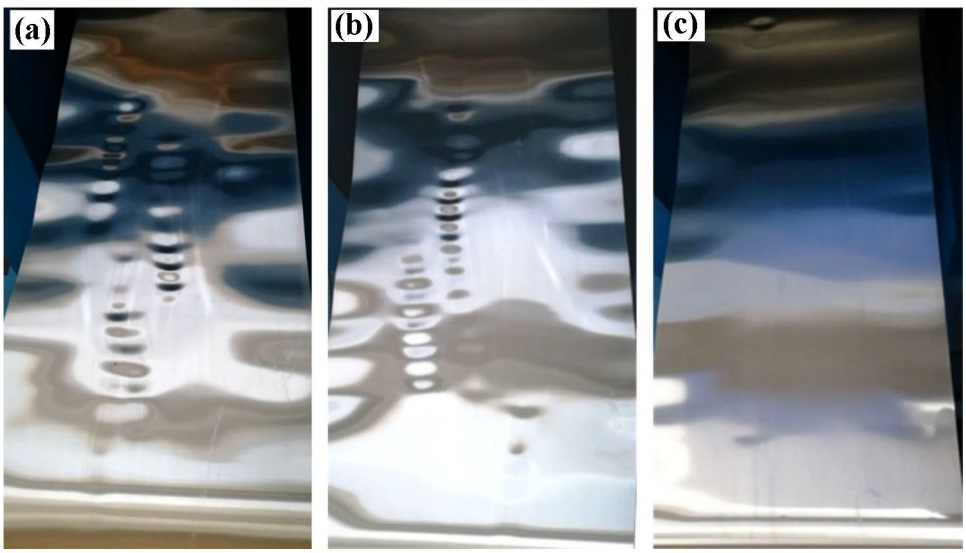

Fig. 18 Strip deformation under different tensions and 15 t rolling forces. Tension is **a** 10 MPa, **b** 20 MPa, and **c** 35 MPa

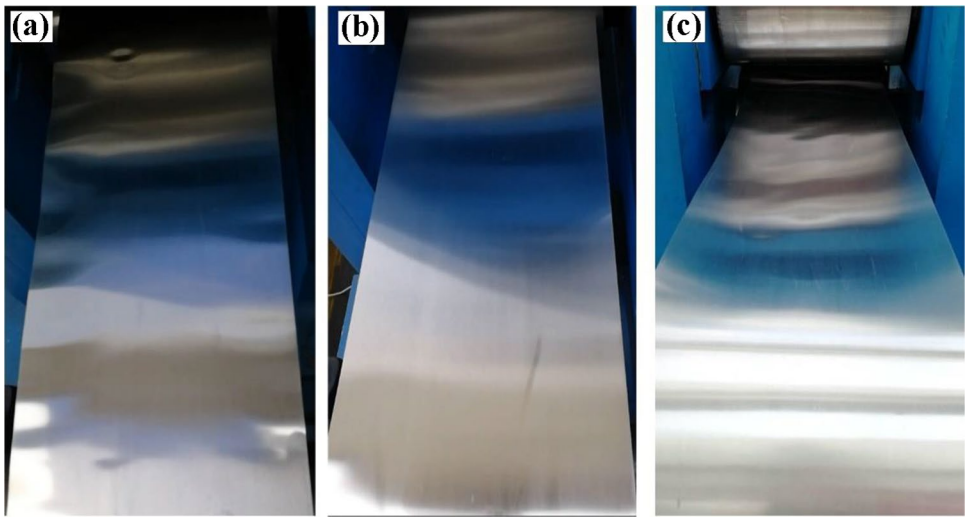

Fig. 19 Strip deformation when C_w is different and D_{UW} is 80 mm. C_w is **a** 0 μm, **b** 30 μm, and **c** 40 μm

4.4 Experimental analysis on the effect of an electromagnetic control rolling mill

Figure 19 shows the strip deformation when C_w is different and D_{UW} is 80 mm. When C_w is 0 μm, noticeable edge waves appear at the strip edge. When C_w is 30 μm, the rolled strip has good strip flatness characteristics, which indicates that the ECR roll profile can compensate for the upper working roll bending better, and the change of roll gap shape is close to each other in the different strip units. When C_w is 40 μm, a slight middle wave is formed in the strip middle. This phenomenon shows that with increasing C_w, the reduction in the strip middle is increased, and the elongation in the strip middle is larger than that at the strip edge. Figure 20 shows the strip distribution of the rolled strip under different C_w when the upper working roll diameter is 80 mm and the tension is 35 MPa. With increasing C_w, the thickness of the strip middle can be decreased, and the thickness of the strip edge can be increased.

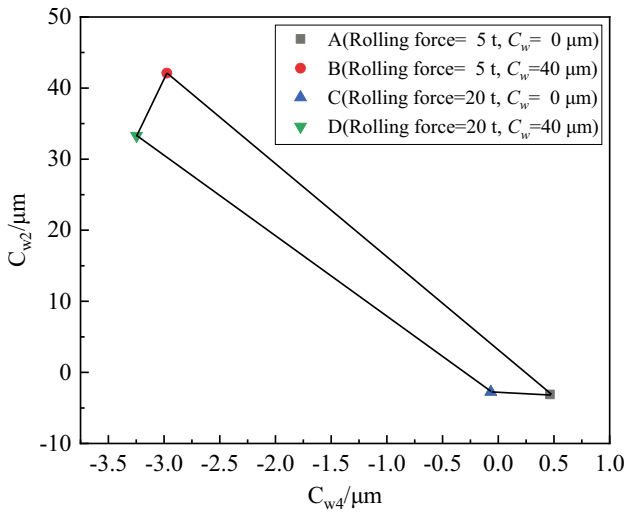

Fig. 20 Strip thickness distribution when C_w is different and D_{UW} is 80 mm

Figure 21 shows the strip deformation when C_w is different and D_{UW} is 120 mm. Due to the increase in D_{UW}, the roll deflection is less than that in Fig. 19. With increasing C_w, the obvious edge wave is changed to the obvious middle wave. The result shows that when C_w is small, the roll deflection is still large under the action of 15 t rolling forces and can result in a considerable reduction at the strip edge. When C_w is increased to a certain value, the reduction amount in the roll gap middle is further increased with increasing C_w, and the elongation in the strip middle is larger than that on the strip edge. The stress distribution of the strip reaches the critical value, and middle wave problems appear. The middle wave in Fig. 21c is more obvious than that in Fig. 19c. The reason is that the stiffness of the upper working roll can be increased with increasing D_{UW}, and the size of the roll gap middle regulated by the microscale roll gap control technology is smaller than that in Fig. 21c, which leads to a more obvious middle wave. Figure 22 shows the strip distribution of the rolled strip when C_w is different and D_{UW} is 120 mm. The variation law of the strip thickness distribution with C_w in Fig. 20 is the same: with increasing C_w, the thickness of the strip middle can be decreased, and the thickness of the strip edge can be increased. Therefore, microscale roll gap control technology has strip flatness control ability.

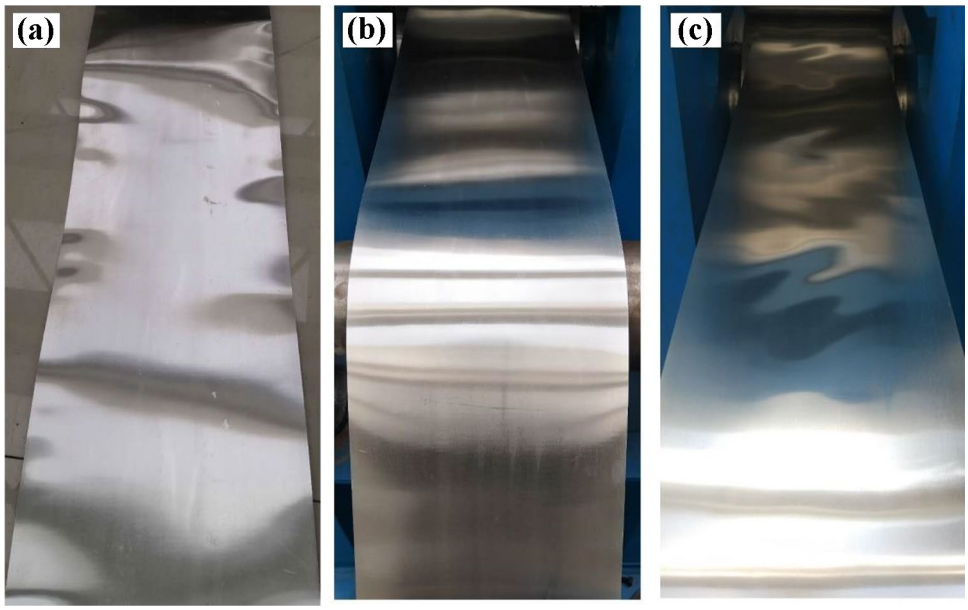

Fig. 21 Strip deformation when C_w is different and D_{UW} is 120 mm. C_w is **a** 0 μm, **b** 30 μm, and **c** 40 μm

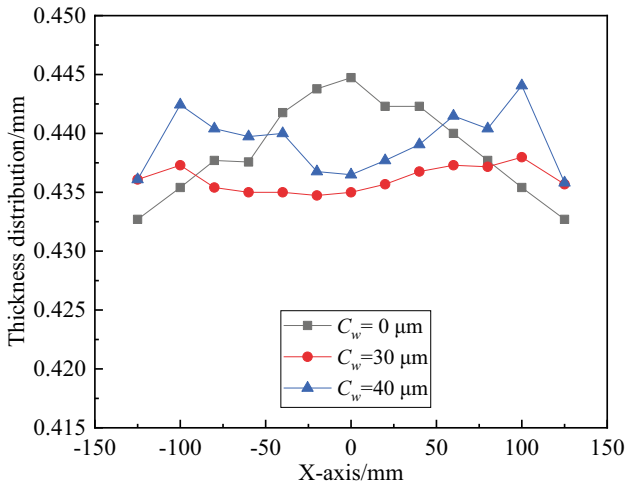

Fig. 22 Strip thickness distribution when C_w is different and D_{UW} is 120 mm

5 Conclusion

This paper proposes microscale roll gap control technology, which can be used to adjust the roll gap shape and control the strip flatness by using an electromagnetic control roll. The conclusions obtained by experiments and simulations are as follows:

(1) Microscale roll gap control technology can improve the strip flatness control ability of rolling mills and directly act on the position of the strip flatness defects to adjust strip flatness and improve strip quality.
(2) Under different rolling forces or different tensions, the average quadratic crown control ability is 40.63 μm or 44.2 μm, and the average quartic crown control ability is − 3.31 μm or − 3.5 μm. Therefore, microscale roll gap control technology has the control ability of quadratic crowns and quartic crowns. The control ability increment of the quadratic crown is greater than that of the quartic crown.
(3) The results of the indentation experiment show that a stable roll gap can be obtained by PID control after the target roll profile is achieved. With increasing regulation amount, the strip crown can be changed from positive to negative under a 10 t or 20 t rolling force. When the rolling force is 30 t, the strip crown can be changed from 19.5 to 0.5 μm, and the effect of the flatness control is also apparent. Therefore, ECR can adjust the strip with edge wave defects to the strip without defects and then adjust it to the strip with middle wave defects.
(4) In the strip rolling experiment, the problem of edge waves can be solved, and strips with good shapes can be obtained. When the ECR roll crown is further increased, the microscale roll gap control technology can adjust the edge wave to the middle wave, proving that the microscale roll gap control technology has considerable control ability for thin strip rolling.

Author contribution Tingsong Yang: conceptualization, methodology, writing—reviewing and editing, formal analysis. Qifa Chen: formal analysis, investigation, writing. Yanfeng Feng: formal analysis, investigation. Yang Hai: conceptualization, methodology. Fengshan Du: funding acquisition.

Funding This project is supported by the National Natural Science Foundation of China (Grant No. U1560206) and National Natural Science Foundation of China (Grant No. 51374184).

Data availability The data sets supporting the results of this article are included within the article and its additional files.

Declarations

Ethical approval Not applicable.

Consent to participate The authors consent to participate.

Consent to publish The authors consent to publish.

Competing interests The authors declare no competing interests.

References

1. Cao JG, Xu XZ, Zhang J, Song MQ, Gong GL, Zeng W (2011) Preset model of bending force for 6-high reversing cold rolling mill based on genetic algorithm. J Cent South Univ 18:1487–1492. https://doi.org/10.1007/s11771-011-0864-6
2. Ogawa S, Hamauzu S, Matsumoto H, Kawanami T (2007) Prediction of flatness of fine gauge strip rolled by 12-high cluster mill. ISIJ Int 31(6):599–606. https://doi.org/10.2355/isijinternational.31.599
3. Wang PF, Zhang DH, Li X, Liu JW, Wang JS (2012) Research and application of non-symmetrical roll bending control of cold rolling mill. Chin J Mech Eng-en 25(1):122–127. https://doi.org/10.3901/cjme.2012.01.122
4. Wang QL, Sun J, Liu YM, Wang PF, Zhang DH (2017) Analysis of symmetrical flatness actuator efficiencies for UCM cold rolling mill by 3D elastic–plastic FEM. Int J Adv Manuf Tech 92(10):1–19. https://doi.org/10.1007/s00170-017-0204-6
5. Wang QL, Sun J, Li X, Liu YM, Wang PF, Zhang DH (2018) Numerical and experimental analysis of strip cross-directional control and flatness prediction for UCM cold rolling mill. J Manuf Process 34:637–649. https://doi.org/10.1016/j.jmapro.2018.07.008
6. Aljabri A, Jiang ZY, Wei Z (2015) Analysis of thin strip profile by work roll crossing and shifting in asymmetrical cold rolling. Int J Mod Phys B 29:10–11. https://doi.org/10.1142/S0217979215400329
7. Lu C, Tieu AK, Jiang ZY (2002) A design of a third-order CVC roll profile. J Mater Process Tech 125:645–648. https://doi.org/10.1016/S0924-0136(02)00373-4
8. Li HB, Zhang J, Cao JG, Meng LL (2011) Analysis of crown control characteristics for SmartCrown work roll. Adv Mater Res 156–157:1261–1265. https://doi.org/10.4028/www.scientific.net/AMR.156-157.1261
9. Li HB (2012) Roll contour and strip profile control characteristics for Quintic CVC work roll. J Mech Eng 48(12):24–30. https://doi.org/10.3901/JME.2012.12.024
10. Linghu KZ, Jiang Z, Zhao J, Li F, Wei D, Xu J, Zhang X, Zhao X (2014) 3D FEM analysis of strip shape during multi-pass rolling in a 6-high CVC cold rolling mill. Int J Adv Manuf Tech 74(9–12):1733–1745. https://doi.org/10.1007/s00170-014-6069-z
11. Fei S, Li H, Kong N, Jie Z, Mitchell DRG (2017) Improvement in continuously variable crown work roll contour under CVC cyclical shifting mode. Int J Adv Manuf Tech 90(9–12):2723–2731. https://doi.org/10.1007/s00170-016-9587-z
12. Cao JG, Wei GC, Zhang J, Chen XL, Zhou YZ (2008) VCR and ASR technology for profile and flatness control in hot strip mills. J Cent South Univ T 15(002):264–270. https://doi.org/10.1007/s11771-008-0049-0
13. Wang XC, Yang Q, Sun YZ (2015) Rectangular Section Control Technology for Silicon Steel Rolling. J Iron Steel Res Int 22(3):185–191. https://doi.org/10.1016/S1006-706X(15)60028-0
14. Li YL, Cao JG, Qiu L, Yang GH, He A, Zhou YZ (2018) Research on ASR work roll contour suitable for all width electrical steel strip during hot rolling process. Int J Adv Manuf Tech 97:1–6. https://doi.org/10.1007/s00170-018-2198-0
15. Cao JG, Chai XT, Li YL, Kong N, Jia SH, Zeng W (2017) Integrated design of roll contours for strip edge drop and crown control in tandem cold rolling mills. J Mater Process Tech 252:432–439. https://doi.org/10.1016/j.jmatprotec.2017.09.038
16. SUMITOMO METAL IND (1994) Shape controller in sheet rolling. JP patent 6015319A:01–25
17. Arif, A.f.M., Ovaisullah Khan., Sheikh, A.K. (2004) Roll deformation and stress distribution under thermo-mechanical loading in cold rolling. J Mater Process Tech 147(2):255–267. https://doi.org/10.1016/j.jmatprotec.2004.01.005
18. Masui T, Yamada J, Nagai T, Nishino T (1983) Strip shape and profile control with a new type of the variable crown roll system. Trans Iron Steel Inst Jp 23(10):846–853. https://doi.org/10.2355/isijinternational1966.23.846
19. Masui T, Matsumoto Y, Tomizawa A, Hirooka E (1992) Variable-crown roll: EP0338172
20. Zhang Q, Wang W, Zhou X (2008) Flatness control behavior of a DSR mill for wide steel strips. J Univ Sci Technol Beijing 01, 71–76. https://doi.org/10.13374/j.issn1001-053x.2008.01.006
21. Du FS, Feng YF, Liu WW, Sun JN, Wang HJ (2017) Measuring technique for roll profile electromagnetic control in precision plate rolling. Iron Steel (11), 80. https://doi.org/10.13228/j.boyuan.issn0449-749x.20170139
22. Liu WW, Feng YF, Yang TS, Du FS, Sun JN (2018) Analysis of the induction heating efficiency and thermal energy conversion ability under different electromagnetic stick structures in the RPECT. Appl Therm Eng 145:277–286. https://doi.org/10.1016/j.applthermaleng.2018.09.043
23. Feng YF, Liu WW, Yang TS, Du FS, Sun JN (2019) A flexible electromagnetic control technique for interference adjustment in large-size sleeved backup rolls. Metall Res Technol 116(4). https://doi.org/10.1051/metal/2018122
24. Stolbchenko M, Grydin O, Samsonenko A, Khvist V, Schaper M (2014) Numerical analysis of the twin-roll casting of thin aluminium-steel clad strips. Forsch Ingenieurwes 3(78):121–130. https://doi.org/10.1007/s10010-014-0182-x
25. Yang TS, Liu JY, Zhou HN, Xu ZQ, Du FS (2021) Analysis of the thermal-force roll profile control ability under different hole structures and slot structures in the RPECT. Int J Adv Manuf Tech 116:403–415. https://doi.org/10.1007/S00170-021-07399-3